

DSF-T-54-97  
ITP-SB-97-69  
HUTP-97/A058  
Revised

# Light masses in short distance penguin loops

Mario Abud <sup>a,b,1</sup>, Giulia Ricciardi <sup>b,c,2</sup>, George Sterman <sup>d,3</sup>

<sup>a</sup>*Dipartimento di Scienze Fisiche, Università degli Studi di Napoli  
Mostra d' Oltremare, Pad 19, I-80125 Napoli, Italy*

<sup>b</sup>*INFN (Sezione di Napoli)  
Mostra d' Oltremare, Pad 19, I-80125 Napoli, Italy*

<sup>c</sup>*Lyman Laboratories, Harvard University, Cambridge, MA 02138, USA*

<sup>d</sup>*Institute for Theoretical Physics, SUNY Stony Brook  
Stony Brook, NY 11794-3840, USA*

## Abstract

Penguin diagrams for decays such as  $b \rightarrow (s, d)\gamma$  involve virtual loops of  $u$  or other light quarks. Logarithms of the virtual quark mass could, in principle, influence the phenomenological analysis of the decay. It is thus important to study these logarithms to all orders in QCD perturbation theory. In this paper we show that, at arbitrary order, the matrix elements of operators in the effective hamiltonian contributing to  $b \rightarrow s\gamma$  are finite for the limit of  $m_u \rightarrow 0$  in penguin loops.

---

<sup>1</sup>*e-mail: mario.abud@napoli.infn.it*

<sup>2</sup>*e-mail: ricciardi@huhepu.harvard.edu*

<sup>3</sup>*e-mail: sterman@insti.physics.sunysb.edu*

# 1 Introduction

In the spectator-quark model, the inclusive weak decays of the  $B$ -meson can be pictured as QCD corrected  $b$ -quark decays. Since in perturbative QCD, virtual light quarks appear in loop diagrams, their presence might suggest an enhancement of the rate through terms involving powers of  $\ln m_{loop}$  (we denote by  $m_{loop}$  the mass of any light quark circulating in the penguin loops). The possible effects of such terms “long-distance” contributions were explored, for example, in Ref. [1]. On the other hand, the finiteness for  $m_{loop} \rightarrow 0$  has been invoked in other papers, such as [2, 3, 4]. In this paper, we address this problem in the context of effective field theory. Our analysis is perturbative and therefore relates to current, rather than constituent quark masses [5].

We refer to a particular flavor changing neutral current process,  $b \rightarrow s\gamma$  decay, but our results can easily be extended to other interesting FCNC processes, such as  $b \rightarrow d\gamma$ . We argue that, to any order in perturbative QCD, the limit  $m_{loop} \rightarrow 0$  in gauge invariant penguin amplitudes is finite, and the presence of virtual light quarks in these internal loops does not result in logarithmic divergences as  $m_{loop} \rightarrow 0$ . To be specific we argue that powers of  $\ln m_{loop}$  are always accompanied by positive powers of  $m_{loop}$  [6]. For example, in  $b \rightarrow (s, d)\gamma$  decays there is a contribution from penguin loops with a virtual  $u$  quark ( $m_{loop} = m_u$ ), but the amplitude does not diverge as  $m_u \rightarrow 0$ . For definiteness, we discuss the exclusive  $b \rightarrow s\gamma$  final state.

Of course, penguin loops are not the only source of dependence on light quark masses. In the partonic  $b \rightarrow s\gamma$  amplitude, subdiagrams involving gluons (photons) attached to the outgoing  $s$ -quark as well as soft gluons attaching the  $b$ -quark with the  $s$ -quark jet, are collinear divergent in perturbation theory in general. In practical calculations, these regions give logarithms of  $m_s$  that are not suppressed by powers of  $m_s$ . In addition, the amplitude for any exclusive final state contains purely infrared divergences associated with the masslessness of the gluon. These kinds of divergence have already been treated in the literature (see for instance [6, 7, 8]). As part of our analysis on penguin loops, we shall show that no additional logarithms arise from light quark loops collinear to the outgoing photon in the particular case of the two-body  $b \rightarrow s\gamma$  decay amplitude. We derive our results by building the effective hamiltonian step by step, showing at each stage which kinds of dependence on light masses are to be expected, and by applying analyticity

arguments and IR power counting techniques developed in perturbative QCD [9].

## 2 The Effective Field Theory

The effective field theory for  $B$ -decays describes the physics at the scale  $\mu \simeq m_b \ll m_W$ , after the top quark and the  $W$  boson have been integrated out. The effective hamiltonian at the lowest order in  $\alpha_{em}$  is defined by a sum of local operators whose matrix elements between initial and final states reproduce the amplitude at low energies

$$H_{eff} = \frac{G_F}{\sqrt{2}} \mathcal{V}_{CKM} \sum_i C_i(\mu) O_i(\mu), \quad (1)$$

where  $\mathcal{V}_{CKM}$  denotes the appropriate factor (typically quadratic in CKM matrix elements). The utility of the effective hamiltonian formalism is that it separates short distance contributions, described by the coefficients, which can be calculated perturbatively, from long distance contributions, incorporated in the matrix elements of the local operators.

We can summarize the steps to build the effective hamiltonian for  $b \rightarrow s\gamma$  as: (i) calculating the coefficients by matching the full theory onto the effective theory at high scale; (ii) evolving the coefficients down to the scale  $O(m_b)$  by the renormalization group (RG) equations; (iii) evaluating the matrix elements of the operators. In the same spirit of Ref. [10], we will analyze the role of the light masses during these three steps.

### 2.1 Matching

The first step consists in matching the effective theory onto the full theory. To match means to extract the coefficients  $C_i$  by comparing the amplitude in the full theory and in the effective theory at the same order in  $\alpha_s$ . At the matching scale, all IR behavior cancels and logarithms of light masses are then eliminated in the coefficients.

As an example, we shall discuss weak penguin diagrams in  $b \rightarrow s\gamma$ , like the one shown in Fig. 1. The effective flavor changing gauge invariant couplings of the photon are of the type  $F_{\mu\nu} \partial^\nu \bar{s}_L \gamma^\mu b_L$  and  $\bar{s}_L F_{\mu\nu} \sigma^{\mu\nu} b_R$ . In a renormalizable theory like the standard model, the corresponding amplitudes must be UV

finite, because the above operators have dimension higher than 4 and cannot arise as counterterms. The amplitude of the full theory, to which the effective theory is matched, can be calculated by expanding in the ratio  $q/m_W$ , where  $q$  is the photon momentum. This expansion can introduce infrared divergences. Since the external photon is taken on shell, the mass of the quark in the loop of Fig. 1 acts as an IR regulator.

The expansion in photon momentum results in terms of the form  $F_1 (q^2 \gamma^\mu - q^\mu \gamma \cdot q)$  and  $F_2 i \sigma^{\mu\nu} q_\nu$ . The form factor  $F_1$  includes an IR-sensitive term  $\frac{2}{3}(x_i - 1) \ln x_i$ , where  $x_i = m_i^2/m_W^2$ , with  $m_i$  the mass of quark  $i$ , circulating in the loop, while in  $F_2 \ln x_i$  appears only multiplied by powers of  $x_i$  (see, for instance, Appendix B of Ref [11]).<sup>1</sup>

In the effective hamiltonian, the local operators contain only light quark fields; the heavy quark fields have been integrated out. In the corresponding diagrams for  $b \rightarrow s\gamma$ , there is an analogous term of the type  $\frac{2}{3} \ln(m_i^2/\mu^2)$ , where  $\mu$  is introduced to fix the scale where the operators are renormalized, through the introduction of a counterterm proportional to  $F_{\mu\nu} \partial^\nu \bar{s}_L \gamma^\mu b_L$ . The coefficients of the effective hamiltonian are found precisely from the difference of the diagrams of the full theory and the corresponding diagrams in the effective theory. If the internal quark is heavy, logarithms of heavy masses will be included in the matching coefficients of the hamiltonian. If the internal quark is light,  $m_i = m_c$  or  $m_u$ , by performing the matching at  $\mu = m_W$  we have an exact cancellation of the term  $\frac{2}{3} \ln x_i$  in the coefficients. In other words, at the matching scale all IR behavior cancels, and the coefficients are manifestly finite for  $m_i \rightarrow 0$ .

## 2.2 RG rescaling

Perturbative QCD corrections introduce logarithms  $\alpha_s^n(\mu) \ln^m(\mu/m_W)$ , with  $m \leq n$ . The RG rescales the coefficients of the effective hamiltonian to scales lower than the matching scale  $m_W$ , and resums such logarithms. After the RG group rescaling, we are left with a residual dependence on the scale  $\mu$ , due to the truncation of the perturbative series. In  $B$ -decays, the first threshold is at  $\mu = m_b$ , and we can stop rescaling at that point; in  $D$  and  $K$  decays one can do a new matching and then use the RG once again to go to a still lower

---

<sup>1</sup>Note, however, that the  $F_1$  term decouples from an on-shell photon with physical polarization.

scale. In any case, if we are to work with perturbation theory, the final scale must be greater than 1 GeV or so. It is self-evident that this step cannot introduce logarithms of light masses.

### 2.3 Matrix elements

The final step consists in calculating the matrix elements of the operators in the low energy theory. In general, matrix elements include loops of virtual light quarks. We will study the limit where the penguin loop quark mass  $m_{loop}$  goes to zero. We want to show that for the specially interesting case of  $b \rightarrow s\gamma$  this limit also does not introduce IR divergences. This implies that, in the final result, any term of the type  $\ln m_{loop}$  will always appear multiplied by powers of  $m_{loop}$  (that is, as  $m_{loop}^a \ln^b m_{loop}$  with  $a > 0$ ). A number of explicit calculations corroborate this expectation; see particularly Ref. [6], where several matrix elements at two loops are calculated.

Let us consider the Feynman diagrams that describe the matrix elements in the effective theory at arbitrary order in QCD perturbation theory. An arbitrary Feynman diagram with  $N$  lines may be written in terms of Feynman parameters as

$$G = \prod_{lines\ i} \int_0^1 d\alpha_i \delta\left(\sum_i \alpha_i - 1\right) \prod_{loops\ r} \int d^4k_r D(\alpha_i, k_r, p_s)^{-N} F(\alpha_i, k_r, p_s)$$

$$D(\alpha_i, l_j, p_s) = \sum_j \alpha_j \left(l_j^2(p_r, k_s) - m_j^2\right) + i\epsilon, \quad (2)$$

where  $l_j$  is the momentum of the  $j$ th line and  $\alpha_j$  its Feynman parameter ( $l_j$  is linear in the loop momenta  $k_r$  and in the external momenta  $p_s$ ). The function  $F$  contains overall factors that do not enter the arguments at this point. This integral can be viewed as a contour integral in a multidimensional complex  $\alpha_j, k_r$  space. In order to find possible logarithms, we have to look for the regions of non-analyticity of the integral. The points of the contour where  $D$  vanishes are called ‘‘singular points’’ (SP’s), and possible singularities of this integral must arise from zeros of the denominator  $D$ . In fact, only certain SP’s, referred to as pinch SP’s, give singularities that cannot be avoided by deforming the integration contours. Necessary conditions for a pinch SP are given by the so-called Landau equations [12].

With each SP is associated a reduced diagram, constructed from the complete graph by simply contracting all lines which are off-shell at the SP. The

reduced diagrams of pinch SP's have a direct physical interpretation [9, 13]. They can be interpreted as a picture of a classical, energy- and momentum-conserving process occurring in space-time, with all internal particles real, on the mass-shell, and moving forward in time. We may turn this interpretation around, in order to identify SP's that are pinched. We select the reduced diagrams associated with an arbitrary Feynman graph that admit such a physical interpretation; these diagrams identify pinch SP's.

Once we have all the reduced diagrams relevant to a particular Feynman graph, we know its sources of non-analyticity. At this stage, it becomes important to have criteria for determining which pinch SP's may actually introduce infrared divergences in the diagram. The presence of pinch SP's reveals the presence of non-analytic terms, such as logarithms of light masses. If these logarithms are suppressed by powers of the light masses themselves, however, the corresponding amplitude will not diverge in the zero-mass limit.

In order to identify possible IR divergences we use IR power counting. An obvious complication for IR power counting in Minkowski space is that  $k^2 = 0$  does not imply  $k = 0$ , so that a naive dimensional counting will not necessarily express the real behavior of the integral in the IR limit. A method for dealing with this problem is to change variables, and approximate the integral near each pinch SP, so that every denominator is a homogeneous function of a set of variables that vanish there [9, 14]. This integral will be referred to as the ‘‘homogeneous’’ integral and these variables as the ‘‘normal’’ variables; the remaining variables, called ‘‘intrinsic’’, parametrize the relevant surface of SP's, and do not contribute directly to the singular behavior. The IR behavior of the homogeneous integral will be determined by dimensional power counting involving only the normal variables. In the following section, we apply the power counting procedure just sketched to  $b \rightarrow s\gamma$ , and verify that the amplitude is free of unsuppressed logarithms of  $m_{loop}$  for  $m_{loop} \rightarrow 0$ .

### 3 The decay $b \rightarrow s\gamma$

The decay  $b \rightarrow s\gamma$  has been extensively studied in the framework of effective field theory [15]. Beyond leading order, the matrix elements of the operators in the effective theory include light quark loops in general. Let us consider one of these diagrams: precisely the penguin diagram in Fig. 2, without QCD corrections. There is a light quark ( $u$ -quark or  $c$ -quark) running in the loop.

We consider the zero mass limit for this quark.

The pinch SP corresponding to the diagram in Fig. 2 is associated with a reduced diagram that coincides with the original one. At the pinch SP, the reduced diagram can be interpreted as a process occurring in space-time, with all internal particles real, on the mass-shell, and moving forward in time. Then it is easy to see that the two light quarks and the photon belong to the same jet, where a jet is defined as a connected set of massless lines, which are on shell with finite energy, and have momenta proportional to a single lightlike momentum ( $p^\mu$  in this case). Therefore, the reduced diagram in Fig. 2 can be viewed as a massive  $b$  quark decaying into two jets, one consisting of the light quark loop and the photon, the other consisting of the  $s$ -quark line only. We use the term “hard” for any vertex of a reduced diagram where lines from two or more jets are attached. We will also refer to on-shell massless lines with zero 4-momentum as soft lines; a “soft subdiagram” is one consisting of only soft lines.

Let us first analyze arbitrary reduced diagrams that contribute to the four-quark operator with two jets,  $J_\gamma$  and  $J_s$ , a single hard part and a soft subdiagram. Fig. 3 shows a typical diagrammatic structure for  $J_\gamma$ ; Fig. 4 shows the general form of these diagrams. Afterwards, we shall treat the remaining, relevant reduced diagrams. The diagrams of Fig. 4 admit a rather simple IR power counting, analogous to the treatment of form factors for quark-antiquark production in  $e^+e^-$  annihilation [9, 14]. An appropriate choice of normal variables for all these processes is the four components  $k_s^\mu$ ,  $\mu = 0 \dots 3$ , of loops  $k_s$  that pass through the soft subdiagram,  $S$ , and the *squares*  $k_j^2$  and  $(k_{s,\perp}^j)^2$  for each loop  $k_j$  that is internal to a jet. For the latter, the transverse momentum is defined relative to the jet’s direction.

The superficial IR degree of divergence related to any reduced diagram of this sort is

$$D = \sum_{i=\{\gamma,s\}} \left( 2L_i - N_i + b_i + \frac{3}{2}f_i + t_i \right), \quad (3)$$

where  $L_i$  and  $N_i$  are the numbers of loops and lines in  $J_i$ , while  $b_i$  and  $f_i$  are the numbers of soft gluons and soft photons attached to  $J_i$  at the pinch SP. The factor  $t_i$  comes from the numerator momenta in  $J_i$  and is bounded from

below<sup>2</sup>,

$$t_i \geq \max \left\{ \frac{1}{2}[u_3^i - v_i], 0 \right\}, \quad (4)$$

where  $u_3^i$  and  $v_i$  are, respectively, the number of three-point vertices in  $J_i$  and the number of soft vector particles attached to  $J_i$ . The Euler identity and counting relations between the numbers of lines and vertices of various orders may then be used to bound the IR degree of divergence by

$$D \geq \sum_{\{i=\gamma,s\}} \left\{ \frac{1}{2}(h_i - 1) + f_i + \frac{1}{2}(v_i - u_3^i)\theta(v_i - u_3^i) \right\}, \quad (5)$$

where  $h_i$  is the number of lines attaching jet  $i$  to the decay vertex. Clearly, the lower limit on  $D$  is found by taking  $h_i = 1$  and  $f_i = 0$ .

We can easily check that for the lowest-order diagram, Fig. 2,  $D > 0$ , because in this case  $h_\gamma = 2$  for the photon jet, which immediately gives  $D = 1/2$ . We may trace the positive value of  $D$  to  $u_3^\gamma = 1$  in Eq. (4). This suppression is a direct result of the transversality of the emitted photon, which requires at least one power of the transverse momentum of the soft quark loop. Therefore, the diagram of Fig. 2 is IR convergent, when the photon is on shell. The all-order power counting expression, Eq. (5) shows that this reasoning holds to any order for diagrams of the form of Fig. 4, since  $h_\gamma = 2$  for all of them when the hard vertex is a four-quark operator.

We can readily extend this reasoning to the remaining pinch SP's that are relevant to  $b \rightarrow s\gamma$ . Further corrections to the four-quark operators are shown in Fig. 5. The only singular points involving an on-shell light quark penguin loop that we have not yet considered are those in which soft gluons attach to the  $b$  quark (Fig. 5a) and those in which the penguin loop itself is soft (Fig. 5b).

First, consider additional gluons attached to the  $b$  quark. The propagator of a quark radiating a soft gluon behaves as  $1/2p \cdot k$  (where  $k$  is the momentum of the gluon) and so contributes  $-1$  to the power counting. For power counting purposes, the  $b$  quark then acts like a third jet in Eq. 3, with no internal loops ( $L_i = 0$ ), no soft external fermions ( $f_i = 0$ ), no numerator suppression ( $t_i = 0$ ), and with the number of its lines equal to the number

---

<sup>2</sup>For this argument, we ignore unphysically-polarized gluon lines that attach the jet to the hard scattering in covariant gauges; they do not affect the overall power counting discussed here [9, 14].



of soft gluons attached to the  $b$  line ( $N_i = b_i$ ). It is easy to verify that pinch SP's of this sort leave Eq. (5) unchanged.

Second, consider the class of pinch SP's for the four-quark operator in which the photon is radiated by the  $s$  (or  $b$ ) quark, and the light quark penguin loop appears as part of the soft subdiagram (Fig. 5b). This diagram is highly suppressed in the IR compared to those of Fig. 5a, because a fermion propagator with momentum  $k^\mu$  diverges only linearly at  $k^\mu = 0$ , in contrast to a boson propagator, which diverges quadratically. Thus, penguin loops, whether connected directly to the photon or not, are finite in the zero-mass limit.

So far, we have restricted ourselves to light quarks in penguin loops only, connected directly to the operators of the effective theory. Mixing of operators in the effective theory, however, gives rise to diagrams in which there is no penguin loop. We will now show that in the two-body amplitude there are no additional logarithms of light quark masses associated with loops in the photon jet, that is, collinear to the outgoing photon.

Consider Fig. 6a, in which the gluon emerges from the hard subdiagram (effectively, the operator  $O_8 \sim m_b \bar{s}_L \sigma^{\mu\nu} T_a b_R G_{\mu\nu}^a$  in the standard classification). These diagrams contain yet another set of pinch SP's, as shown, in which this gluon changes into a photon due to rescattering of a loop of virtual light quarks with soft gluons. We may once again use the power counting of Eq. (5), but this time  $h_\gamma = 1$ , and on a diagram-by-diagram basis, the amplitude produces logarithms of the light quark mass. Note that charge conjugation invariance requires at least two soft gluons attached to the quark loop (two C-odd gluons cannot produce a C-odd photon), so that this effect appears first at three loops in the perturbative matrix element. Nevertheless, the contribution from any SP of this sort cancels in a gauge invariant set of diagrams, because the photon does not carry color. This result follows from the factorization of soft gluons from jets, an important ingredient in factorization proofs for inclusive cross sections [16, 17].

Leaving technicalities aside, soft gluons can couple only to the total color charge of a jet. In fact, the contribution of the SP of Fig. 6a may also be pictured as in Fig. 6b, which shows that the total effect of the soft gluons is to insert a nonabelian phase factor in the color product between the decay vertex and the gluon line. The double line represents the nonabelian phase; the relevant Feynman rules are described, for example, in [17]. Here, however, it is only the topology of the figure that is important. The remaining jet in

Fig. 6b consists of a gluon and a photon, connected by the light quark loop, whose color trace vanishes identically. Let us note that this factorization does not require a sum over final states; indeed, the cancellation of soft gluons in inclusive processes in Refs. [16, 17] requires the factorization as a first step, for each final state individually. Thus, logarithms of  $m_{loop}$  associated with these processes are absent, since, as we have just seen, a gluon cannot fragment by interacting only with soft quanta. Note that this reasoning does not apply to final states describing the collinear splitting of the gluon into a photon plus other gluons.

In summary, we have shown, to all orders in  $\alpha_s$  and to the lowest order in  $\alpha_{ew}$ , that penguin-like diagrams relevant for the process  $b \rightarrow s(d)\gamma$  can be safely calculated by taking the massless limit for the  $u$ -quark circulating in the penguin loop. This implies, for instance, that no large “enhancements” (i. e. IR unsafe contributions) in the amplitudes involving the CKM matrix elements  $V_{ub}V_{ud}^*$  are expected from this source at any fixed order in perturbation theory. We have also observed that in the perturbative expansion of the two-body final state, no logarithms of light-quark masses arise from loops collinear to the outgoing photon.

## Acknowledgements

We wish to thank Howard Georgi, Tobias Hurth, Michelangelo Mangano and A. Soni for helpful conversations. We would also like to thank Z. Ligeti and J. Soares for useful communications. G.R. thanks the Institute for Theoretical Physics at Stony Brook for its hospitality. This work was supported in part by the National Science Foundation, under grants PHY9722101 and PHY9218167.

## References

- [1] N.G. Deshpande, X.-G. He and J. Trampetic, Phys. Lett. B 367 (1996) 362.
- [2] A. Ali and C. Greub, Phys. Lett. B287 (1992) 191.
- [3] J. Soares, Phys. Rev. D49 (1994) 283.

- [4] A. Ali, preprint DESY 95-157, hep/ph 9508335, Proceedings of the XXXth Rencontres de Moriond “Electroweak Interaction and Unified Theories”, Les Arcs, France, March 1995.
- [5] D. Atwood, B. Blok, A. Soni, Nuovo Cimento 109 A (1996) 873.
- [6] C. Greub, T. Hurth and D. Wyler, Phys. Lett. B380 (1996) 385; Phys. Rev. D54 (1996) 3350.
- [7] A. Ali and C. Greub, Phys. Lett. B 259, 182 (1991); Phys. Lett. B 287 (1992) 191; Phys. Lett. B 361, 146 (1995); N. Pott, Phys. Rev. D54 (1996) 938.
- [8] A. Kapustin, Z. Ligeti and H.D. Politzer, Phys. Lett. B357 (1995) 653.
- [9] G. Sterman, Phys. Rev. D17 (1978) 2773.
- [10] G. Ricciardi, Phys. Lett. B355 (1995) 313.
- [11] T. Inami and C.S. Lim Progr. Theor. Phys. 65 (1981) 297; 1772E.
- [12] L.D. Landau, Nucl. Phys. 13 (1959) 181.
- [13] S. Coleman, R.E. Norton, Il Nuovo Cimento 38, Ser. 10 (1965) 438.
- [14] G. Sterman, *An Introduction to Quantum Field Theory*, (Cambridge Univ. Press, Cambridge, 1993), Ch. 13.
- [15] M. Ciuchini, E. Franco, G. Martinelli, L. Reina and L. Silvestrini, Phys. Lett. B316 (1993) 127, Nucl. Phys. B421 (1994) 41; M. Misiak Nucl. Phys. B393 (1993) 23, E B439 (1995) 461 E; G. Cella, G. Curci, G. Ricciardi and A. Viceré, Phys. Lett. B325 (1994) 227; Nucl. Phys. B431 (1994) 417; M. Misiak, M. Münz, Phys. Lett. B344 (1995) 308; K. Chetyrkin, M. Misiak and M. Münz, Phys. Lett. B400 (1997) 206; C. Greub and T. Hurth, Phys. Rev. D56 (1997) 2934; K. Adel and Y.-P. Yao, Modern Physics Letters A8 (1993) 1679; Phys. Rev. D49 (1994) 4945; A. Ali, and C. Greub, Z.Phys. C49 (1991) 431.
- [16] J.C. Collins and G. Sterman, Nucl. Phys. B185 (1981) 172.
- [17] J.C. Collins, D.E. Soper and G. Sterman, in *Perturbative Quantum Chromodynamics*, ed. A.H. Mueller (World Scientific, Singapore, 1989).

## Figure Captions

- Fig. 1 One of the penguin diagrams of the full theory, as computed, for example, in Ref. [11].
- Fig. 2 Penguin diagram of the effective (low energy) theory.
- Fig. 3 Typical reduced diagram for the QCD corrections to the penguin-like diagrams.
- Fig. 4 General reduced diagram for soft gluon corrections to the  $b \rightarrow 2$  jets transition.
- Fig. 5a Same as Fig. 4, but with gluonic insertions in the  $b$ -quark line.
- Fig. 5b Reduced diagram, analogous to those of Figs. 4, 5a, but with the  $\gamma$  arising from an external ( $b$  or  $s$ ) quark line, instead of the light quark loop.
- Fig. 6a Reduced diagram with a gluon arising from the hard vertex. The sub-diagram hard gluon  $\rightarrow$  soft gluons +  $\gamma$  vanishes by color conservation (see text).
- Fig. 6b Factorization of the soft gluon contribution to the diagram of Fig. 6a. The double line represents the nonabelian phase referred to in the text.

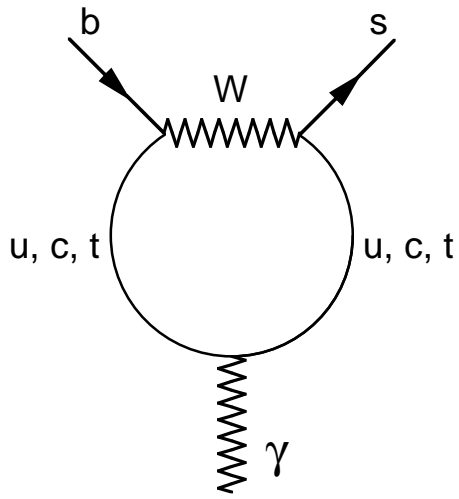


**Fig.1**

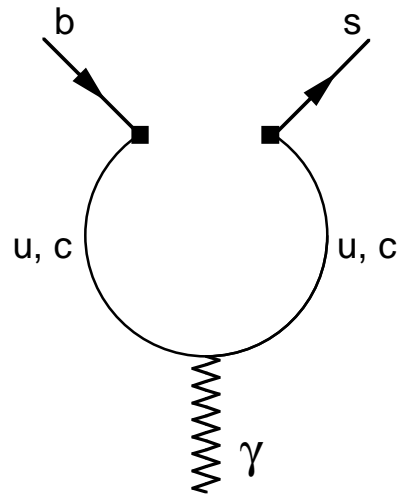


**Fig.2**

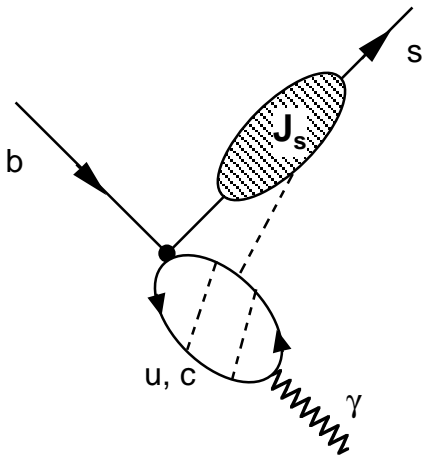


**Fig.3**

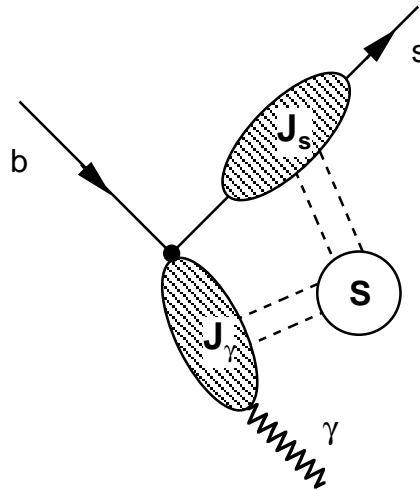


**Fig.4**

The hard vertex is represented by the black disk.  
 The dashed lines are gluons.  
 The blobs  $J_s$  and  $J_\gamma$  indicate the  $s$  and  $\gamma$  jets respectively.

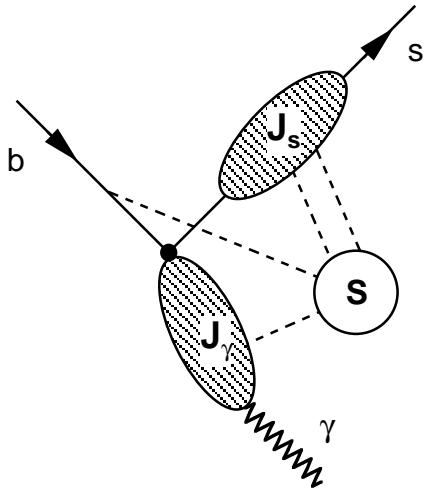


Fig.5a

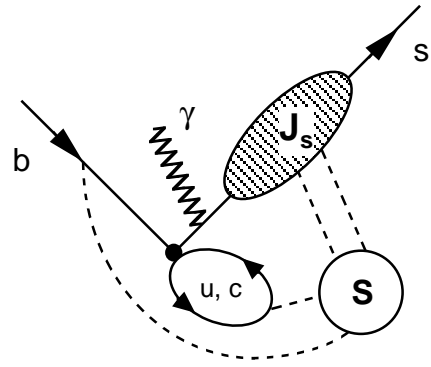


Fig.5b

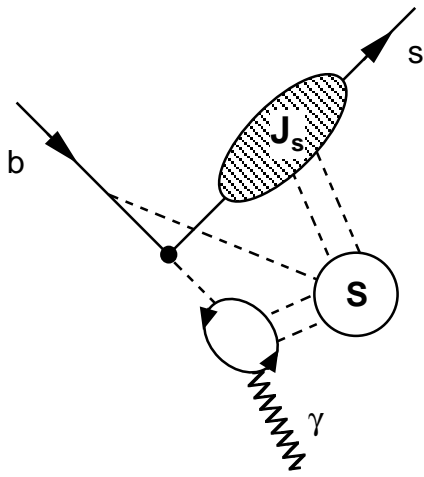


Fig.6a

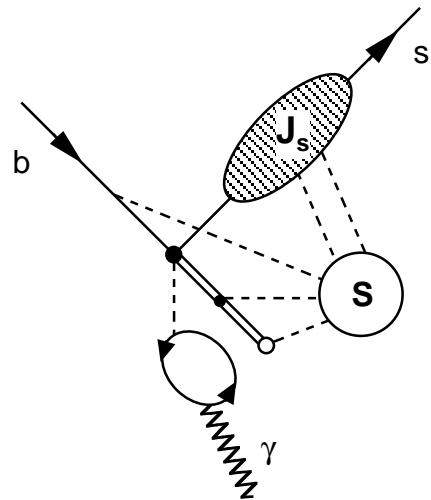


Fig.6b

The hard vertex is represented by the black disk.  
 The dashed lines are gluons.  
 The blobs  $J_s$  and  $J_\gamma$  indicate the  $s$  and  $\gamma$  jets respectively.  
 The double line of Fig.6b represents a non abelian phase.